



Survey and Monitoring of Relativistic Electrons in Petawatt Laser Shots - Some Options

JE Bateman, MJ Mead

September 2013

©2013 Science and Technology Facilities Council



This work is licensed under a [Creative Commons Attribution 3.0 Unported License](https://creativecommons.org/licenses/by/3.0/).

Enquiries concerning this report should be addressed to:

RAL Library
STFC Rutherford Appleton Laboratory
Harwell Oxford
Didcot
OX11 0QX

Tel: +44(0)1235 445384
Fax: +44(0)1235 446403
email: libraryral@stfc.ac.uk

Science and Technology Facilities Council reports are available online at: <http://epubs.stfc.ac.uk>

ISSN 1358-6254

Neither the Council nor the Laboratory accept any responsibility for loss or damage arising from the use of information contained in any of their reports or in any communication about their tests or investigations.

SURVEY AND MONITORING OF RELATIVISTIC ELECTRONS IN PETAWATT LASER SHOTS – SOME OPTIONS

J.E.Bateman,

Science and Technology Facilities Council, Rutherford Appleton Laboratory, Harwell
Science and Innovation Campus, Didcot, Oxfordshire, OX11 0QX, U.K.

M. J. Mead

Horia Hulubei National Institute of Research & Development in Physics and Nuclear
Engineering, 30 Reactorului Street, Magurele, Ilfov, Romania.

23 September 2013

Abstract

The exciting products of petawatt laser shots, charged particles and gamma rays of energies up to 100MeV and attosecond light pulses depend on the primary production of relativistic electrons (i.e. with energies comparable to or greater than the electron rest mass). On the negative side, recent work at Lawrence Livermore National Laboratory [1] and recent analysis by the present authors [2, 3] points the finger at the flux of high energy (MeV) electrons leaving the target as the cause of the damaging electromagnetic pulse (EMP) frequently associated with such shots. Monitoring the magnitude and distribution of these electrons within a shot is clearly desirable. This report discusses the problems associated with this procedure and proposes some relatively simple detector systems appropriate to the task. Passive, dynamic and time domain detector types are considered using both the Cerenkov and scintillation processes. The Cerenkov type is shown to provide the maximum differentiation between electron flux and the other types of radiation present.

1. Introduction

The scientific case for the Extreme Light Infrastructure (ELI) [4] is predicated on the ability of petawatt laser pulses delivered in picosecond pulses to generate high energy x-rays ($>1\text{MeV}$), energetic ion beams (e.g. protons $>100\text{MeV}$) and ultra-short (attosecond) light pulses as well as electron beams of multi-MeV energies. All of these processes are dependent on the production of very hot ($>\text{MeV}$) electrons in the primary plasma which escape from the target region in copious ($>10^{12}$) quantities. The analysis presented in a previous report [2] demonstrated that the electron spectra observed at LLNL [1] could be approximated as the sum of two quasi-thermal distributions of high energy electrons with temperatures of (in a typical shot) 0.53MeV and 12.6MeV and that relativistic effects caused the shell of electrons to bunch up into a fast pulse of a few tens of picoseconds wide.

Follow-up studies [3] showed that a further relativistic effect (the compression of the electric field of a moving charged particle) made the interaction of this pulse with any metal surface it encountered extremely impulsive (again on a sub-nanosecond timescale). This analysis points strongly to the interaction of the electron pulse with the chamber structure as the source of the very high, impulsive electric fields observed generally in petawatt laser shots, known as the electromagnetic pulse (EMP). Thus study of the relativistic electron flux escaping from the target would seem to be a profitable avenue of research into the generation and mitigation of the often extremely destructive EMP. Since the fast electrons are intrinsic to many processes of interest in high power laser studies, the value of diagnostic measurements of their properties can be expected to confer many benefits beyond EMP studies.

The measurements described in reference [1] in which magnetic spectrometers are used, have given excellent data on the energy spectrum and spatial distribution of the fast electron fluxes from laser shots. However, the technologies used are complex and are not adapted to routine or dynamic (i.e. on a shot-by-shot basis) measurement such as could form a part of any target facility. In this report we investigate technologies (adapted from nuclear physics) which could provide routine diagnostics for the fast electron production of any experiment.

The environment created by a typical petawatt laser shot is extremely challenging for any radiation detector.

- A large number of particles ($\sim 10^{12}$) are created on a very short time scale (picoseconds), though flight times spread them to nanosecond time scales at typical detector distances (0.5m – 1m) from the target.
- The expanding shell of particles comprises not only the fast electrons but electromagnetic radiation of all wavelengths from (keV) x-rays to (MeV) gamma rays. Also present are target ions, which if hydrogen is present can result in protons of MeV energies. These radiations propagate throughout the target chamber and therefore interact with any device or material present.
- The presence of very high electric fields from the EMP can threaten the integrity of any electronic device within the chamber and make live-time data recording difficult.

Three distinct modes of operation seem relevant.

- Passive survey, in which cheap simple detectors can be placed ad libitum around the target chamber and the distribution of relativistic electrons monitored by recording on

a retrievable medium for analysis off-line – probably after several shots as the chamber must be opened up to retrieve them.

- Active monitoring, in which a signal proportional to the electron flux through the detector is available external to the target chamber with each shot.
- Time domain analysis, in which a fast detector system provides a time profile of the electron flux at the chamber location where the detector is situated.

Clearly the active modes of detection are most useful since the electron fluxes change with the parameters of the shot (as shown clearly in the results of reference [1]). However, as will appear, this mode presents many technical challenges.

Two primary detection processes are considered to meet the conflicts intrinsic to the requirements outlined above. Both involve the use of plastic light-generating materials, primarily to reduce the sensitivity of the detectors to the wide energy range of x-rays and gamma rays in the environment (as noted below, the stopping power of a material for high energy electromagnetic radiation is a strong function of the atomic number (Z) over most of the energy range of interest). For the purposes of the study the two detector systems envisaged have sensitive elements consisting of a disk of polymethylmethacrylate - PMMA or Perspex - (the Cerenkov detector) or plastic scintillator 2.5cm diameter and 3mm thick. At a distance from the target of 50cm this equates to a solid angle of $1.96 \cdot 10^{-3}$ steradians (str) and 3mm of plastic equates to the extrapolated range of ~ 0.8 MeV electrons. As a typical flux of electrons ($T > 0.5$ MeV) is $\sim 10^{11}$ / str, this translates to $\sim 2 \cdot 10^8$ relativistic electrons passing through the detector in a single laser shot.

2. The Cerenkov Detector

A fast charged particle emits light (Cerenkov radiation [5]) whenever its velocity (v) exceeds the velocity of light in the optical medium through which it is travelling i.e. $v > c/n$ where c is the free-space luminal velocity and n is the refractive index of the material. Thus the process has a well-defined threshold for any given particle given by $\beta = 1/n$ where $\beta = v/c$. Relativistic kinematics translates this condition (using $\gamma = 1/\sqrt{1-\beta^2}$ where γ is the ratio of the total relativistic energy of the particle to its rest mass) to:

$$T_T = \left(\frac{1}{\sqrt{1-\frac{1}{n^2}}} - 1 \right) m_0 c^2 \quad (1)$$

Where $m_0 c^2$ is the rest mass of the particle expressed in terms of energy, (for an electron this is 0.511MeV) and T_T is the kinetic energy that the particle must exceed to generate the radiation. In Perspex around a wavelength (λ) of 500nm, $n = 1.49$ and for electrons $T_T = 0.178$ MeV. The light is emitted in a shock cone at an angle to the particle track of θ such that $\cos \theta = 1/\beta n$ with a spectral distribution given by:

$$\frac{d^2 N}{dx d\lambda} = \frac{2\pi\alpha}{\lambda^2} \sin^2 \theta \quad \text{per particle}$$

where dN/dx is the number of photons generated per unit length of track and α is the Fine Structure Constant : $1/137$.

dN/dx is determined by integrating this equation over the wavelength range detected which is usually determined by the light detector used. Inserting the constants and using units of nm for λ gives:

$$\frac{dN}{dx} = 4.59 \cdot 10^5 \left(\frac{1}{\lambda_1} - \frac{1}{\lambda_2} \right) \sin^2 \theta \quad \text{photons/cm} \quad (2)$$

Adopting the wavelength band appropriate to silver halide film and the standard photocathode (S11) ($\lambda_1 = 350\text{nm}$ and $\lambda_2 = 500\text{nm}$) and substituting $\cos \theta = 1/\beta n$ gives:

$$\frac{dN}{dx} = 393.4 \left(1 - \frac{1}{\beta^2 n^2} \right) \text{photons/cm} \quad (3)$$

And $\beta^2 = 1 - 1/\gamma^2 = 1 - 1/(1+T/m_0c^2)^2$ where T is the electron kinetic energy.

For electrons of sufficient energy, (>1MeV in Perspex) the light output becomes asymptotic at ~ 200 photons/cm. Below this energy one must integrate expression (3) just over the portion of the electron track in which $T > T_T$ using the range-energy relation relevant to the particle and material.

Figure 1 shows the results of the calculation of the total number of photons produced in a number of radiators as a function of the electron energy (right hand Y-axis in the figure). To show the relevant region of sensitivity of the Cerenkov process, one of the electron energy spectra derived from reference [1] is superimposed (dN/dT - the double negative-exponential curve in the figure). Along with the curve for 3mm Perspex, those for 10mm of three aerogels of different density are presented. The availability of these aerogels [6] offers the opportunity to adjust the electron energy threshold upward if desired.

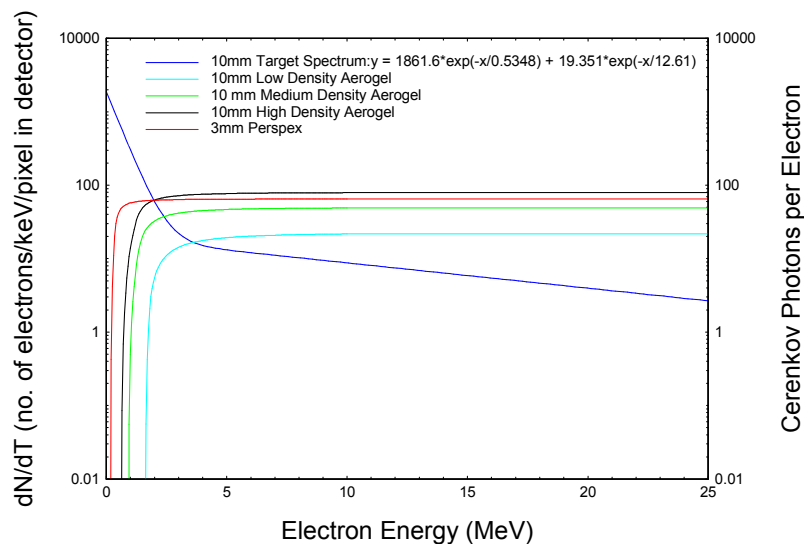


Figure 1: The estimated number of Cerenkov photons per electron as a function of electron energy.

For an estimate of the order of magnitude of the light pulse from a single shot, we assume a mean output of 50 photons/electron which, given 2×10^8 fast electrons hitting the detector, results in a total signal of $\sim 10^{10}$ photons per shot.

2.1 Passive Survey Detector

In certain experimental phases in high power laser studies the ability to survey the fast electron flux over large portions of the target chamber may be highly desirable. A cheap and simple device which can be used in large numbers called for. Such a device can be realised by wrapping a strip of standard silver halide (AgX) film around the edge of a Perspex disk such as is specified above. The two planar faces can be thinly coated with a suitable diffuse reflector (e.g. aluminium oxide) to randomise the light paths of the Cerenkov photons and direct them towards the active edges. The area of the film is 1.88cm^2 so that if (as one would expect) a substantial fraction of the photons reach the film, then the exposure on the film is $\sim 5 \times 10^9/\text{cm}^2$. This is probably adequate to give a useful optical density in one or two shots.

The AgX emulsion is of course sensitive to ionising radiation such as the electrons. However it is very thin and will generally be positioned so that its edge faces the target and present a very small solid angle to anything originating there. Any signal generated in it can readily be calibrated out by wrapping a second shrouded strip around the first one, developing both together and taking a differential measure of the optical density.

The housing for the disc and film can be very simple and should be convenient to load and unload in the dark room. It should be fabricated from low density, low Z material to minimise the generation of secondary radiation.

Some form of calibration is highly desirable and this can be accomplished relatively simply by the use of a collimated radioactive source which emits a pure high energy beta spectrum e.g. $^{90}\text{Sr}/^{90}\text{Y}$ ($T_{\text{max}} = 2.27\text{MeV}$).

In the case of over-sensitivity, attenuation of the Cerenkov light is easily arranged with filters. In the case that more sensitivity is required there is an option to reduce the effective λ_1 in equation (2) as far as the UV absorption edge of the Perspex and ensure that the latter is of the UV-transparent variety. By coating the readout edge with a very thin layer of wavelength shifter (typically $50\mu\text{g}/\text{cm}^2$ of P-Terphenyl) the UV component can be shifted into the blue region and an enhancement of a factor of 2 to 3 in the detected photons obtained. Finally, the sensitivity can be controlled (approximately over a decade) by selection of the speed of the film stock used.

The electron discrimination properties of this detector are very good which is important in the radiation-rich environment of the target chamber. Target ions are not a problem (the threshold for protons in Perspex is 327MeV). But the large flux of gamma rays generated in the target plasma is more problematic since it can generate fast electrons within the Perspex by Compton scattering and (above 1.02MeV) by pair production. The Compton electrons have a maximum energy $T_c = E_\gamma/(1 + 0.511/2E_\gamma)$ MeV which is about 80% of E_γ at 1MeV . Only electrons with energies between T_T and T_c are available to generate Cerenkov photons which reduces the effective efficiency of the detector for gammas. Figure 2 shows a simple estimate of the effective conversion efficiency of 3 mm of Perspex (in Cerenkov mode) as a function of gamma (x-ray) energy and compares it with the values that would be experienced by a

scintillation detector which has no threshold. The clear result is that the Cerenkov detector is immune to x-rays up to about $E_\gamma = 0.3\text{MeV}$ and above that has a maximum sensitivity of 1.8%. This calculation does not take account of the fact that the Cerenkov signal takes a further 1MeV of energy to reach saturation output, so that in terms of Cerenkov photons the peak in the signal is less pronounced than shown.

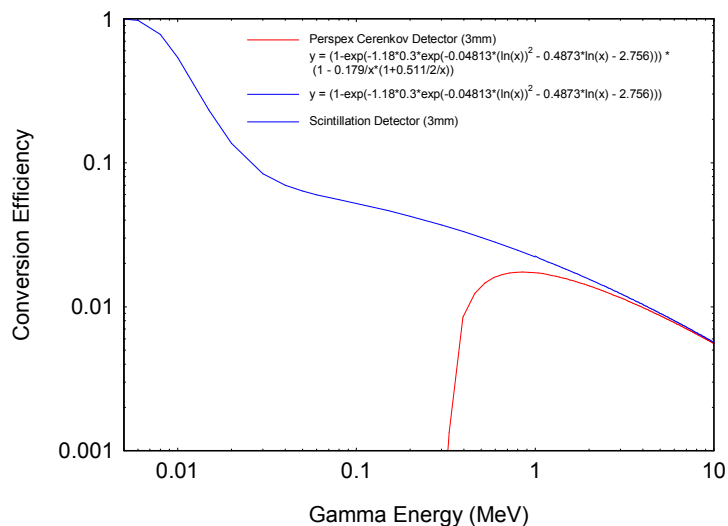


Figure 2: Estimate of the x-ray/gamma ray conversion efficiency of the Cerenkov detector with the Scintillation detector for comparison.

2.2 Dynamic Detector

Clearly a detector system producing an electronic readout on a shot by shot basis would be highly desirable since the passive detector system requires the target chamber to be opened for retrieval of the films. The quantity of photons available in a shot ($>10^9$ photons) would represent a generous signal for detection in a laboratory environment. However, the harsh environment of the target chamber would make operation of a conventional photo-detector difficult and expensive because of the large radiation flux and the EMP problem. It is therefore attractive to consider the possibility of using a completely electrically passive connection to the disk in the form of a flexible light pipe which couples the radiator disc to a remote photo-detector which is easily shielded from both the EMP and ionising radiation.

A suitable product for this application is one of the large diameter, flexible plastic fibre optic produced by Anchor Optics [7]. In this case the 3mm diameter fibre optic would be appropriate to be optically glued to a flat on the edge of the Perspex radiator disc. The cable is very flexible (minimum bending radius 24mm) and has an attenuation of 0.8dB/m over a spectral range of 380nm to 750nm which translates to a halving of the signal in $\sim 4\text{m}$. Since the fibre is close coupled to a material with the same refractive index as the core the parameter determining the acceptance is the trapping angle which is calculated to be 19deg. In order to maximise the fraction of rays within this cone, the radiator disc is coated overall in high reflectivity diffuse reflector. Estimating the efficiency of trapping in the fibre is not a simple matter but a lower bound can be estimated from the solid angle subtended by the fibre at the centre of the disc as $\sim 0.5\%$. The diffuse reflector will increase this by a significant

factor for which a conservative estimate of 2 will be taken giving a trapping efficiency of $\sim 1\%$ which reduces our pulse of 10^{10} photons to 10^8 per shot.

The fibre is made of the essentially similar material to the radiator disc. Depending on where the detector is located in the chamber, the fibre will be exposed to a significant flux of fast electrons through it which will in turn generate Cerenkov light within the fibre. Because of the trapping condition only a small fraction of this will be directed towards the photo-detector. However, if the length of the fibre in the chamber space is long a significant signal could be generated which will be very position dependent. In order to circumvent this problem it is necessary to perform a differential measurement (as in the passive detector case above) by running a second identical blind fibre attached to the active one and reading it out simultaneously so that any fibre contribution can be subtracted.

With a signal of the order of 10^8 photons delivered in a few nanoseconds, there are many options available for the fibre readout which can be chosen with reference to individual experimental requirements. For the purposes of demonstration a simple photodiode with charge-sensitive amplifier is given. In this case, with a suitable simple pulse-shaping post amplifier, a pulse of typically microsecond width is delivered for analysis by standard analogue to digital conversion and storage. A high quality photodiode such as the Hamamatsu S3590-08 [8] coupled to the Hamamatsu SD-37 charge amplifier [8] would perform well with an RMS noise of ~ 300 electrons. Assuming a $\sim 50\%$ loss in the fibre with a photodiode quantum efficiency (QE) of $\sim 50\%$ the signal recorded would correspond to $>10^7$ electrons at the preamplifier input with a noise of <1000 electrons Full Width at Half Maximum (FWHM) i.e. 0.001% . With a signal of this magnitude it is probably possible to use a standard cheap photodiode such as the Vishay BPW21R [9] which has a 3mm active area well matched to the fibre. The specification indicates that the noise would rise by a factor of ~ 10 and the effective QE fall by a factor of 2 but the signal to noise ratio would still be very good.

For a survey instrument with many channels, readout via a large area CCD imaging chip can be considered where the image area can accommodate a large number of fibres placed in close proximity. A standard SLR camera body with the lens replaced by a frame supporting a fibre bundle could possibly provide automatic digitisation of the light signals with suitable triggering of the exposure control.

2.3 Time Domain Measurement

The timing resolution of the Cerenkov detector is ultimately set by the transit times of particles and light in the radiator disk. The corresponding path lengths are mm and tens of mm respectively setting the resolution in the region of a few tens of picoseconds. There is geometric time dispersion in the fibre optic which is estimated to be in the order of 74ps RMS per m. Very fast photodetectors are available in the *sensL* MicroFM silicon photomultipliers series with response times of 0.4ns FWHM with the 0.25mm device and 0.7ns FWHM with the 1mm (square) device [10]. At least an order of magnitude of signal would be lost adapting to the smaller areas but these devices can operate with gains of 10^4 , more than compensating for the signal loss and the statistical quality of the pulse would still be quite adequate based on the figures analysed above.

Figure 3 shows the estimated time of flight (TOF) spectrum for the electrons from a typical laser shot at a distance of 1m from the target. The ill-conditioned nature of the transform from TOF to electron energy means that the finite time resolution on any measurement limits the usefulness of the TOF as a measure of the electron energy spectrum except at low energies ($< 1\text{MeV}$, i.e. $\text{TOF} > \sim 3.5\text{ns}$). If longer flight paths are available with adequate particle flux then the TOF can become more useful. The time domain measurement is an additional diagnostic which may be useful in cases of anomalous or disrupted shot.

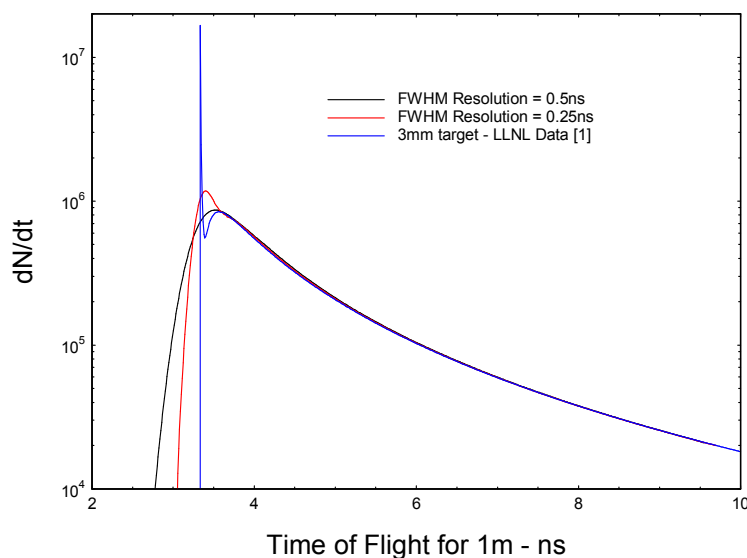


Figure 3: Time of Flight spectrum for a 1m path for a typical fast electron energy spectrum from reference [1, 2] with photo-detector time resolution convolved.

3.0 The Scintillation Detector

The replacement of the Perspex disc by a geometrically identical one of plastic scintillator such as one of the BC-400 series (Saint-Gobain Crystals [11]), changes the detection situation in two important respects: first, the light signal is dramatically increased (by a factor of ~ 500) and secondly, the detector becomes sensitive to the full range of ionising radiation impinging on it – x-rays, gamma rays, electrons and ions with no possibility of discrimination. The main problem is the inability to separate the x-ray/gamma ray component from the relativistic electrons which all arrive at the detector within an interval of a few nanoseconds. As figure 2 shows, the scintillator is sensitive to low x-ray energies where we may always expect a strong x-ray flash from the target. Absorbing this before the scintillator will in general require considerable stopping power (particularly with high Z laser targets) which will distort the electron spectrum and will also generate spurious fast electrons from the gamma flux. However, the large increase in light output makes all forms of readout simpler to manage; in particular the dynamic readout described in section 2.2 above can be simplified as there would be no need for a compensating readout channel on each fibre and smaller diameter fibres could be used so making a global CCD readout encompass many more channels.

Figure 4 shows the typical energy deposit expected from fast electrons in 3mm of scintillator. The cusped curve is the simple-minded estimate from the projected range data while the upper curve is a more realistic estimate derived from a Monte-Carlo model [12] which takes account of the intense scattering that the stopping electrons experience. The output is proportional up to $T_e = 0.9\text{MeV}$ and settles back slowly above this value as T_e increases.

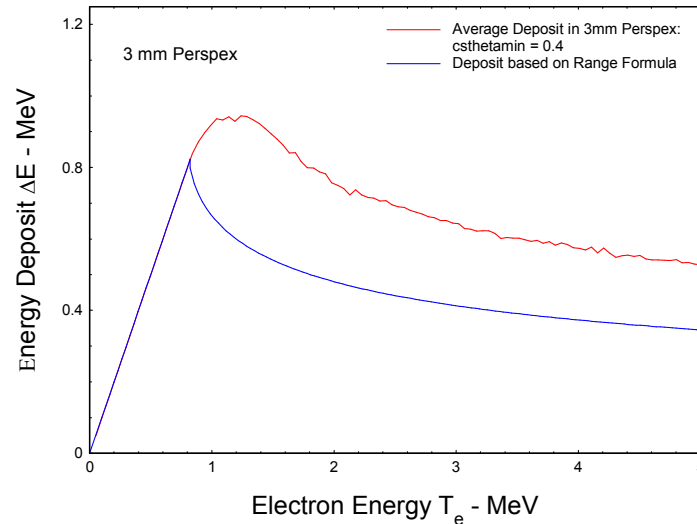


Figure 4: Estimate of the energy deposit of a fast electron in 3mm of plastic as a function of the electron energy.

The scintillator BC-404 (for example) has a light output of 0.68 that of anthracene ($1.5 \cdot 10^4$ photons/MeV [13]) i.e. essentially 10^4 photons/MeV. From Figure 4 we can set $T_e = 0.6\text{MeV}$ as a rough average of an electron energy deposit, giving 6000 photons per electron and with $2 \cdot 10^8$ electrons per shot, $1.2 \cdot 10^{12}$ photons per shot. Such deposits of energy, $\sim 10^8$ MeV in just 1cc (1g) of scintillator in a few nanoseconds is far in excess of typical experience in nuclear physics and it is possible that some saturation effects may occur. If this magnitude of signal is safely delivered by the scintillator then the readout options for both passive and dynamic survey/monitoring systems (while the same in principle) are given wider options than the Cerenkov case. However, the problem of separating the x-ray/gamma ray signal remains.

In the time domain, the scintillator cannot offer much in the context of electron TOF analysis; BC-404 (the fastest of the series) has a FWHM of the light pulse of 2.2ns. As figure 3 shows such resolution would be of little value. The x-ray and gamma ray signal would arrive exactly on top of the high energy ($> 1\text{MeV}$) in which we are interested. However, the stopping power of 3mm of scintillator for protons is 15.8 MeV. The energy deposit curve for the protons will look very similar to the cusped plot in figure 4 with the peak at 15.8MeV and the energy deposit above this proton energy dropping slowly after the initial dip. The slowness ($1/v$) of protons ranges from $\sim 70\text{ns/m}$ at 1MeV to 7ns/m at 100MeV so any significant proton flux will appear above the low energy electron TOF distribution seen in figure 3 at longer TOF values. Heavier target ions will travel correspondingly slower and be easily resolved at times which could stretch into microseconds.

4.0 Conclusions

The schema of a detector system has been presented which permits the survey and monitoring of the fast (relativistic) electron flux from petawatt laser shots. Based on the unique sensitivity of the Cerenkov detection process to relativistic charged particles, it guarantees maximal differentiation between the electron flux and that of other ionising radiations present. The technology is relatively simple with survey modules read out by means of silver halide film wrapped around them and developed off-line and the dynamic (shot by shot) modules delivering a light pulse via a fibre optic cable to a photo-detector safely remote from the harsh environment of the target chamber. This pulse is an integrated signal containing information from all electrons of energy greater than the Cerenkov threshold (0.178MeV for electrons in a Perspex radiator) resulting from the laser shot.

The possibility of using the scintillation process instead of the Cerenkov process was also discussed. Giving a very substantially greater signal, the scintillation process, on the other hand, has the drawback of responding to all forms of ionising radiation which impact it. This makes it unsuitable for reliable electron detection. However, equipped with a fast photo-detector and operated in the time domain it could offer the ability to give information on the ion spectrum by means of time-of-flight measurements.

References

- [1] Mitigation of Electromagnetic Pulse (EMP) Effects from Short-Pulse lasers and Fusion Neutrons, D C Eder, A Throop, C G Brown Jr., J Kimbrough, M L Stowell, D A White, P Song, N Back, A MacPhee, H Chen, W DeHope, Y Ping, B Maddox, J Lister, G Pratt, T Ma, Y Tsui, M. Perkins, D O'Brien and P Patel, LLNL-TR-411183 (2009)
- [2] J E Bateman and M J Mead, Rutherford Appleton Laboratory Report: RAL-TR-2012-005 Available as e-publication at www.stfc.ac.uk
- [3] J E Bateman and M J Mead Rutherford Appleton Laboratory Report: RAL-TR-2012-021 Available as e-publication at www.stfc.ac.uk
- [4] www.extreme-light-infrastructure.eu
- [5] Cerenkov Radiation, J V Jelley, Pergamon, London 1958
- [6] L Cremaldi, D A Sanders, P Sonnek, D J Summers and J Reid Jr., IEEE Trans Nucl. Sci, June 2009, arXiv:0905.3411v1 [physics.ins-det] 20 May 2009
- [7] www.anchoroptics.com/catalog
- [8] www.hamamatsu.com
- [9] <http://uk.rs-online.com>
- [10] www.sensl.com
- [11] www.detectors.saint-gobain.com
- [12] J E Bateman, Nucl. Instr. and Methods B184 (2001) 478
- [13] The Theory and Practice of Scintillation Counting, J B Birks, Pergamon, London 1967